9

Research Article

Raed Sattar Jebur* and Raad Hamdan Thaher

Design and simulation of photonic crystal fiber for highly sensitive chemical sensing applications

https://doi.org/10.1515/eng-2022-0562 received September 05, 2023; accepted November 12, 2023

Abstract: Photonic crystal fibers (PCF) have demonstrated promising capabilities for liquid sensing applications owing to their distinctive optical properties. This work presents a numerical investigation of a PCF sensor optimized for discriminating water, ethanol, and benzene samples. In the proposed configuration, there are five concentric rings of air holes in the cladding arranged in a hybrid lattice structure, while the core contains only one air hole. The optical properties of the sensor, such as refractive index, power fraction, relative sensitivity, confinement loss, effective area, and nonlinearity, were assessed through a comprehensive analysis utilizing the full vector Finite Element Method within the COMSOL Multiphysics software. All these properties have been meticulously examined through numerical investigation across a broader range of wavelengths spanning from 0.8 to 2.2 μm . The suggested model has high sensitivity, minimal confinement loss, and an exceptional nonlinear coefficient value. At a wavelength of 1.3 µm, the suggested PCF exhibits greater sensitivity of 96.84, 98.12, and 100% for water, ethanol, and benzene, respectively, and nonlinear coefficients of 13.98 W⁻¹ km⁻¹ for water, 13.93 W⁻¹ km⁻¹ for ethanol, and 14.85 W⁻¹ km⁻¹ for benzene, with decreased confinement loss. The created model can be utilized in several research areas, particularly in chemical sensing and bio-sensing, as well as their respective applications.

Keywords: chemical sensor, confinement loss, nonlinearity, photonic crystal fiber, relative sensitivity

e-mail: eeph008@uomustansiriyah.edu.iq

Raad Hamdan Thaher: Department of Electrical Engineering, University Mustansiriyah, Baghdad, Iraq, e-mail: raadthaher55@gmail.com

1 Introduction

Over the past few years, significant attention has been given to broadening the potential uses of Photonic Crystal Fiber (PCF) technology. PCFs have ushered in a new age by overcoming many of the constraints of traditional optical fiber. PCFs have introduced new epochs to the history of optical technology by allowing for design freedom [1]. Two categories of fibers are classified based on the mechanism they use to guide light. The first type is effective index guiding PCF, with a solid core and air holes positioned randomly or in a regular pattern in the cladding region. The air holes in the cladding of index guiding PCFs have an effective refractive index lower than that of the solid core. The second optical fiber category is photonic-bandgap guiding PCF. This type of fiber can regulate light guiding across all frequency bands. Light confinement has occurred in the core area of the lower refractive index as compared to the cladding [2].

Through adjusting air hole size, shape, and location, PCF technology enables precise customization of the propagation characteristics of the fiber. Changing the geometry parameters may produce Different PCF guiding characteristics [3]. The remarkable properties of PCF have attracted attention from researchers and industries alike. PCF has proven to be a versatile technology with applications beyond its initial communication use. For instance, it has been used in imaging, security, and astronomy, as evidenced by various research studies [4,5]. Additionally, PCF can be applied in different chemical and biological detection areas, including liquid, pressure, mechanical, and temperature sensing [6–11]. The technology works by injecting various test analytes into the core air holes of the fiber, making it a valuable tool for different industries.

One of the most common applications of PCF in sensing is as a chemical sensor. The design of these sensors has undergone significant evolution over the years, thanks to pioneering research by an assemblage of scientists. Scientists developed diverse PCF designs for varied applications. A variety of applications in environmental protection, industrial process control, health and safety, security,

^{*} Corresponding author: Raed Sattar Jebur, Department of Electrical Engineering, University Mustansiriyah, Baghdad, Iraq,

medicine, and scientific research are made possible by liquid identification sensors [10]. For these application cases, it is essential to accurately discriminate between even closely related liquids, such as water—ethanol—benzene.

Numerous studies have explored different arrangements and forms of PCF to utilize them in various applications for sensing purposes. One group of researchers [12] evaluated a hexagonal PCF design with three cladding rings and seven air holes in the core, which achieved modest sensitivity levels of 24.2, 23.3, and 24.9% for detecting ethanol, water, and benzene, respectively. Asaduzzaman and colleagues [10] headed a different group that suggested a sensor with a circular lattice structure. The sensor contained three layers of air holes surrounded by cladding and a core with oval-shaped gaps. This design achieved a 29% relative sensitivity in detecting ethanol. Reference [9] presented a hexagonal grid PCF sensor with a single-core elliptical hole and four cladding air hole layers, achieving a relative sensitivity of 41.37% for water detection. Ahmed and Morshed [13] proposed a PCF configuration for detecting liquids, which featured a hexagonal arrangement of five cladding rings and a core comprising nine holes in an array of elliptical shapes. This design demonstrated significant relative sensitivities for detecting ethanol, water, and benzene, with values reaching as high as 46.9, 45.1, and 47.4%, respectively. Another research team [14] proposed a sensor that detects chemical analytes such as water, ethanol, and benzene, showing a relative sensitivity of 48.2, 53.2, and 55.6%, respectively. Ahmed et al. [15] reported a PCF chemical sensor featuring a cladding structure comprising five circular apertures arranged in an octagonal pattern and a core with nine square-shaped holes, achieving relative sensitivities of 56.8% for ethanol, 52.1% for water, and 58.9% for benzene. Additionally, all test analytes exhibited a confinement loss of around 10⁻⁵ dB/m. In reference [16], a PCF design was introduced, featuring elliptical core holes and three cladding air hole rings. This design demonstrated relative sensitivities of 62.6, 65.3, and 74.5% for detecting water, ethanol, and benzene. The PCF exhibited low confinement losses of 10^{-7} , 10^{-8} , and 10^{-11} dB/m for each liquid. Another research team [17] proposed a PCF structure for chemical sensing with a circular PCF design consisting of a hexagonal core and five outer cladding rings, which demonstrated exceptional relative sensitivities of 88.9, 91.9, and 97.9% for water, ethanol, and benzene, respectively. This PCF design also exhibited low confinement losses of 10⁻¹⁰ dB/m for all tested analytes. Finally, reference [18] reported relative sensitivities of 94.5, 96.3, and 99.6% for water, ethanol, and benzene, respectively. Additionally, all test analytes exhibited a low confinement loss. These studies demonstrate the potential of PCF for sensing applications, with different designs and configurations achieving varying sensitivity levels for different target analytes.

In the past, researchers have focused on designing intricate and complicated PCF structures involving multiple layers of cladding holes, complex core designs, and using elliptical or hexagonal holes to achieve optimal simulated optical properties. However, these elaborate designs can lead to complex manufacturing processes, which increases the risk of manufacturing defects and inaccuracies in hole size. The complexity of these structures also makes them challenging to fabricate. It can result in errors in individual air holes that can affect neighboring air holes, causing challenges in creating complex systems with several air holes and intricate fiber core structures [19–21]. So, we need a simple PCF structure that balances the PCF's essential performance features and its ease of manufacturing. The suggested design has 90 circle air holes in five layers of cladding and one liquid-infiltrated circular hole in the core. This study focuses on optimizing a new hollow-core PCF's photonic crystal cladding microstructure to maximize sensitivity to the target analytes. The effects of varying hole size, pitch, and the number of rings are numerically modeled to relate the structure to sensitivity performance. This is followed by an experimental demonstration of discrimination between water, ethanol, and benzene using the optimized PCF sensor. The sensor specificity, accuracy, and limits of detection are quantified. The terahertz frequency range is essential in scientific research, notably in the detailed investigation and analysis of chemical and biological entities using specially designed sensors [22]. So, this study investigates these properties across the infrared range of 0.8-2.2 µm using water, ethanol, and benzene as analytes for testing.

This research aims to develop, simulate, and analyze a liquids identification sensor based on PCF to distinguish and detect water, ethanol, and benzene. A numerical optimization approach will enhance the optical response to liquids by optimizing the PCF geometry. The anticipated results will establish design principles for engineering PCFs tailored for specific liquid analyte detection applications.

2 Method

In this study, we developed a new high-sensitivity, low-confinement loss hollow-core PCF for chemical sensing. To evaluate the performance of the fiber, we carried out both experimental measurements and numerical simulations. The method section of this article is divided into two subsections: chemical sensor geometry and numerical analysis.

2.1 Chemical sensor geometry

The basic working principle of PCF sensors involves the substance being analyzed, located in the propagation core region, and affecting the optical signal [23]. The PCF is an essential component of these sensors, which has an evanescent field of light that can extend up to the analyte for detection. The cladding air holes play a vital role in keeping the light confined to the core region for optimal light-analyte interaction. Figure 1 displays a transverse cross-sectional view of the proposed PCF design in this study comprised of three layers: a core infiltrated with liquid, cladding with air holes, and a Perfectly Matched Layer (PML). The core is responsible for conducting light, the cladding restricts light inside the core region, and the PML absorbs the leaking wavelength to prevent the reflection of light back into the cladding.

The proposed design for selective chemical sensing is located in the hollow circular hole in the fiber's core, indicated by its diameter dc. The cladding is composed of numerous air holes distributed over its area, with the outermost three rings consisting of 54 circular holes with a size of d that are spaced equidistantly at a distance of p. The fourth ring has 12 circular holes with a diameter of d_1 and a distance of p_1 between each hole, while the final ring nearest to the core has 24 circular holes with a diameter of d_2 arranged equidistantly at a distance of p_2 . To prevent the reflection of wandering waveguides onto the fiber, a Perfectly Matched Layer (PML) is used beyond the cladding zone. The proposed PCF design aims to create a fiber that is easy to manufacture by using circular holes that are

considered simple to produce. Before finalizing the design, these holes' diameter and pitch size are adjusted to the appropriate dimensions.

The suggested PCF sensor is designed with a cladding composed of air holes. The outer three layers of the cladding are made up of holes with a diameter of $d=2~\mu m$ and a pitch distance of $p=2.2~\mu m$. The two layers nearest to the core have smaller hole diameters of $d_1=0.8~\mu m$ and $d_2=0.5~\mu m$, with distances between each hole of $p_1=1~\mu m$ and $p_2=0.7~\mu m$, respectively. The center of the fiber has a circular hole with a diameter of dc = $4.1~\mu m$, which can be filled with various liquid analytes. To satisfy the boundary criterion, the total diameter of the fiber is $24~\mu m$, and the Perfectly Matched Layer (PML) has been adjusted to have a size equivalent to 10% of the diameter of the cladding.

2.2 Numerical analysis

To analyze the performance of the proposed PCF design, a simulation was conducted using the COMSOL Multiphysics software version 5.5 and the full-vector Finite Element Method (FEM). A finer meshing type was employed to ensure accurate design mapping, resulting in a mesh comprising 372 vertex elements, 3,710 edge elements, and 35,694 triangular elements. The degrees of freedom for the mesh were found to be 278,231. The eigenvalue solver error was determined to be 9.5×10^{-8} , indicating high accuracy in the simulation results. The 2D Wave Optics Module was employed to investigate the characteristics

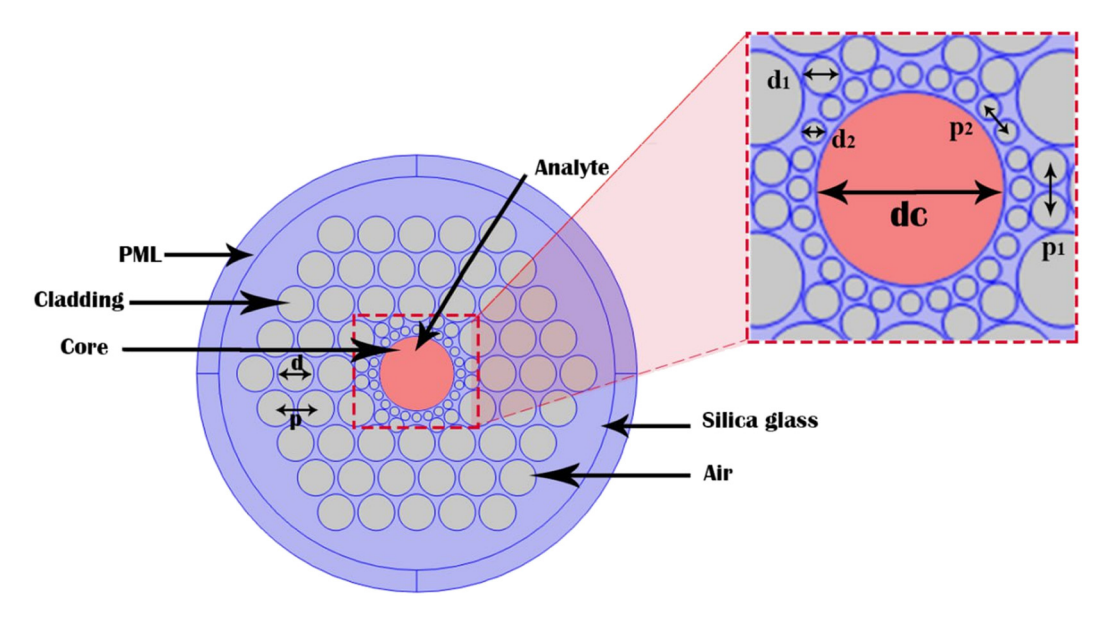


Figure 1: Suggested PCF model for chemical detection.

of electromagnetic waves, specifically focusing on frequency domain physics and mode analysis. Figure 2 illustrates the sequential steps in designing PCF using the COMSOL Multiphysics software.

The study focused on a specific domain of wavelengths, from 0.8 to 2.2 μ m. The PCF architecture was identified as a suitable candidate for liquid sensing applications due to its ability to accommodate different liquids for detection purposes. To evaluate the sensing capabilities of the proposed PCF, the study selected three specific liquid analytes, namely water, ethanol, and benzene. To determine the refractive indices of these analytes for the relevant wavelengths, the study employed Table 1, which displays the index of refraction for each sample for the corresponding wavelengths [16]. Therefore, the study aimed to evaluate the potential of the PCF for liquid sensing by analyzing its response to specific analytes.

Various optical parameters have been examined to evaluate the feasibility and efficiency of the suggested PCF design. These parameters include effective refractive index, relative sensitivity, power fraction, confinement loss, and effective area. These parameters are studied to assess the design's capability to detect the liquid analytes. The overall feasibility of the design for practical applications has also been assessed based on these parameters. Through the evaluation of these optical parameters, a

Table 1: Refractive index vs wavelength (µm) of analyte

Wavelength	Water (RI)	Ethanol (RI)	Benzene (RI)	
0.8	1.3290	1.357	1.4853	
0.9	1.3280	1.356	1.4828	
1.0	1.3270	1.355	1.4810	
1.1	1.3255	1.354	1.4798	
1.2	1.3240	1.353	1.4788	
1.3	1.3225	1.353	1.4781	
1.4	1.3210	1.352	1.4775	
1.5	1.3190	1.352	1.4770	
1.6	1.3170	1.351	1.4776	
1.7	1.3145	1.351	1.4777	
1.8	1.3120	1.350	1.4775	
1.9	1.3090	1.349	1.4774	
2.0	1.3060	1.348	1.4773	
2.1	1.3010	1.347	1.4772	
2.2	1.2960	1.346	1.4773	

comprehensive understanding of the proposed PCF design's capabilities can be achieved, allowing for optimization and potential improvements to be made to enhance its practicality and effectiveness.

A separate liquid is pumped into an additional core hole in the background material, which is formed of silica. Sellmeier's equation may be used to simulate the effective refractive indices n_{eff} [16,24]:

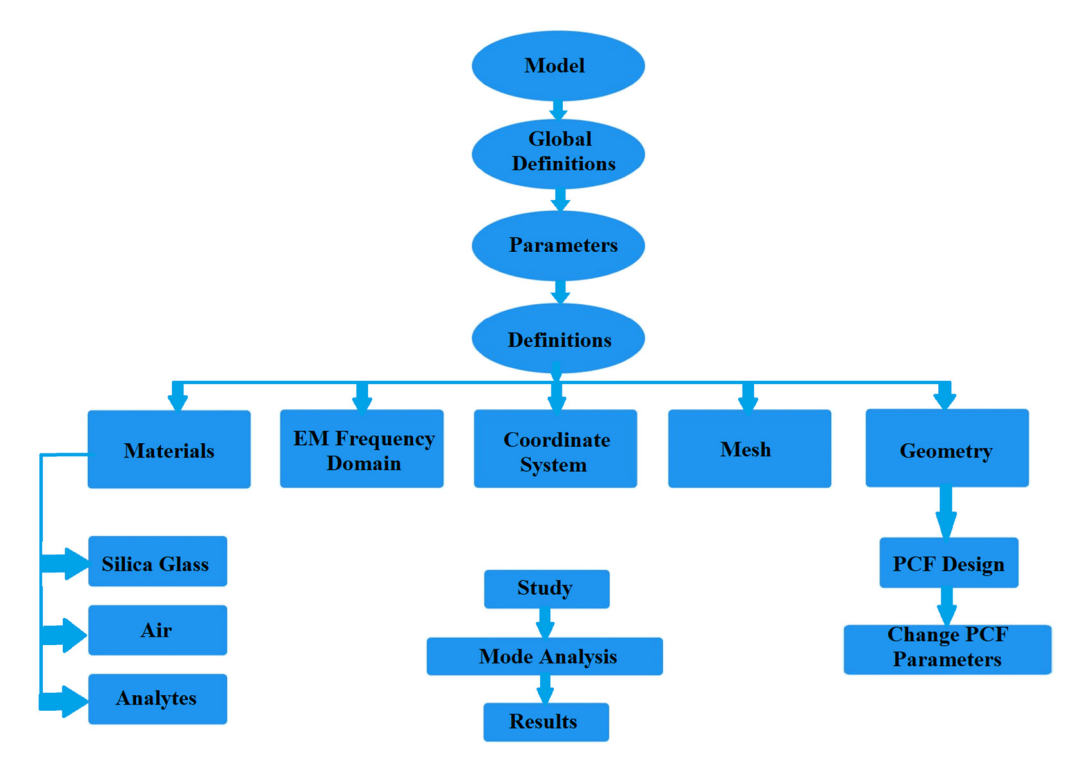


Figure 2: Procedural steps in designing the PCF within the COMSOL Multiphysics tool.

Here, Sellmeier coefficients specific to the material are represented by B_i and C_i (i = 1, 2, and 3), while the working wavelength is denoted by λ .

To assess the PCF sensor's ability to detect analytes, its relative sensitivity (S) is calculated by comparing the refractive indices of the analyte and the surrounding medium and measuring the amount of light that interacts with the analyte. The equation used to calculate relative sensitivity is [16,25,26]:

$$S = \frac{n_{\rm r}}{n_{\rm off}} \times f. \tag{2}$$

This equation shows the relationship between the material's refractive index that is being detected (n_r) , the modal refractive index (n_{eff}) , and the power fraction (f) of the detected material. The power fraction is characterized as the ratio of power in a chemically loaded area to the overall power in the entire fiber and is determined through integration. This metric indicates the quantity of energy transmitted across the PCF at a given location. Poynting's theorem is used to derive this equation [25-27].

$$f = \frac{(\text{sample}) \int \text{Re}(E_x H_y - E_y H_x) dx dy}{(\text{total}) \int \text{Re}(E_x H_y - E_y H_x) dx dy} \times 100,$$
 (3)

where the guided mode's transverse electric and magnetic fields are denoted as E_x , E_y , and H_x , H_y , respectively. This statement means that the integral in the numerator of the equation covers the area of the fiber where the analyte is present, specifically the fiber's core, while the denominator covers the entire area of the fiber.

The PCF design displays confinement loss, which is light leakage from the core into the cladding region. The fiber's structural features cause this confinement loss. To determine the confinement loss, one must calculate the imaginary component of the complex effective index, which can be obtained by utilizing the subsequent equation [9,28,29]:

$$L_{\rm c} = 8.686 \times \frac{2\pi f}{c} \text{Im}(n_{\rm eff})(\text{dB/cm}). \tag{4}$$

This equation calculates the confinement loss in the PCF and involves the operating frequency (f), the speed of light (c), and the imaginary part of the effective refractive index $Im(n_{eff})$.

To calculate the effective area of the fiber core A_{eff} , the transverse electric field vector of the entire cross-sectional area of the PCF is used. The effective mode area is related to the effective area of the fiber core, which is the part of the core that can transport light. The equation used to calculate the effective area of the fiber core is [26,30,31]:

$$A_{\text{eff}} = \frac{\left(\iint_{-\infty}^{\infty} |E|^2 dx dy\right)^2}{\iint_{-\infty}^{\infty} |E|^4 dx dy},$$
 (5)

where E represents the transverse electric field vector. Large effective mode areas are needed in systems that transmit data at high bit rates.

The effective area of the fiber is directly related to nonlinearity ν , also known as the nonlinear coefficient. It is a measurement of how well a fiber can contain highintensity light [31]. It is possible to define as [25,28]:

$$\gamma = \left(\frac{2\pi}{\lambda}\right) \left(\frac{n_2}{A_{\text{eff}}}\right),\tag{6}$$

where the nonlinear refractive index n_2 and the operational wavelength λ are both present. To compute the nonlinearity, the nonlinearity index of SiO₂ is used as $n_2 = 3.2 \times 10^{-20} \text{ m}^2/\text{W}$.

3 Results and discussion

Various performance metrics, such as confinement loss, effective area, nonlinearity, relative sensitivity, and power fraction, have been examined for water, ethanol, and benzene to assess the efficacy of the suggested PCF design for sensing analytes. At an operating wavelength of 1.3 µm, the core region of the fiber is where the interaction of light takes place, and the mode field is entirely confined to all three test analytes: water, ethanol, and benzene. Figure 3 depicts the fundamental x-polarized mode profiles of the three penetrated analytes (water, ethanol, and benzene) in the core at a wavelength of 1.3 µm.

In general, the significant confinement of light within the core of a single air hole confirms the effectiveness of the proposed design in guiding waves. This confinement also suggests a strong interaction between light and analytes, crucial for achieving high sensitivity in liquid detection. By optimizing the power fraction and intensity within the hollow core, one can achieve the ideal alignment between the guided modes and the infiltrated liquids, thus maximizing their overlap.

The experimental results demonstrate that the effective refractive index of the analyzed materials decreases as the operating wavelength increases, which is consistent with the theoretical predictions based on the chromatic dispersion of the refractive index. The refractive index of optical materials inherently reduces at longer wavelengths

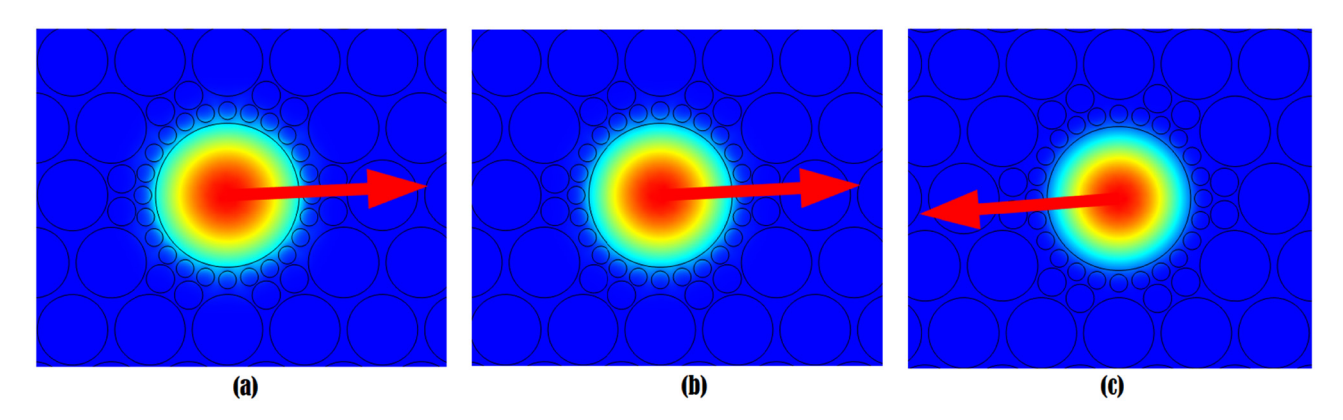


Figure 3: Mode profiles within the proposed PCF structure of (a) water, (b) ethanol, and (c) benzene.

due to the dispersive nature of the interaction between light and matter. The suggested PCF configuration exhibits the same trend demonstrated in Figure 4. The effective refractive index is reduced because tiny electromagnetic waves experience this phenomenon when they travel through a high refractive index area. Additionally, it was discovered that water has the least effective refractive index, while benzene and ethanol have the highest out of the analytes examined.

The peak sensitivities for water and ethanol detection occur at 1.1 μ m wavelength (Figure 5), indicating this is the optimal operating point for discerning these liquids. This wavelength matches the evanescent field penetration depth for efficient sampling of the analyte. While benzene sensitivity monotonically decreases with wavelength, operation

at 1.3 µm provides a balance of adequate sensitivity and low loss, as observed in (Figure 7).

In summary, an operating point of 1.3 μ m provides near-optimal sensitivity for all three analytes while minimizing loss. The proposed single-hole core PCF sensor demonstrates sensitivity rivaling more complex geometries, highlighting the efficacy of the simple design.

It is important to note that the sensitivity measurement is influenced by how the core is structured and the refractive index of the liquid being sensed. Thus, the recommended wavelength for obtaining the highest sensitivity is $1.3 \mu m$, with the polarization of the incident light in the *x*-direction. This particular wavelength will likely provide the most accurate and precise detection of liquid samples, especially for water and ethanol.

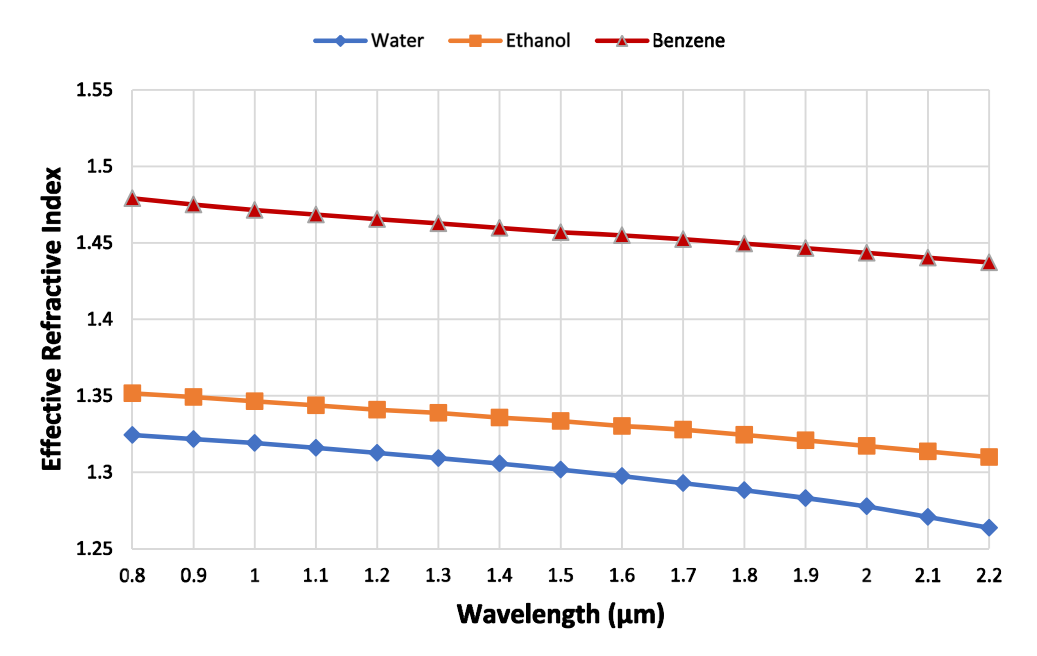


Figure 4: Changes in the effective refractive index of the fundamental x-polarized mode based on the wavelength for liquid analytes.

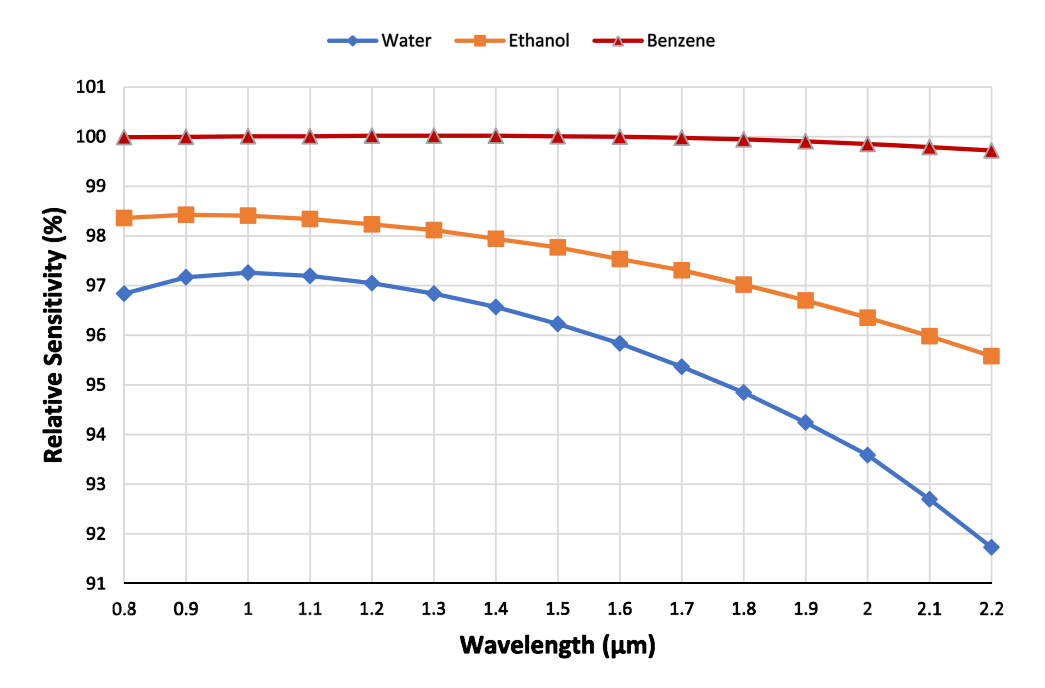


Figure 5: Changes in the relative sensitivity of the fundamental x-polarized mode based on the wavelength for liquid analytes.

The study reports that the proposed PCF has significantly higher relative sensitivities for detecting water, ethanol, and benzene than those reported in references [9,10,12–18]. Specifically, the relative sensitivities for water, ethanol, and benzene are 96.84, 98.12, and 100% greater than those listed in those references. The study also measured other waveguide characteristics at the same *x*-polarization

axis since the sensitivity levels were higher in this polarization direction.

Figure 6 presents the power fraction and wavelength correlation in the PCF sensor. It indicates that the power fraction of water and ethanol increases as the wavelength increases to a plateau at around 1.0 μm before gradually decreasing. In contrast, the power fraction of benzene

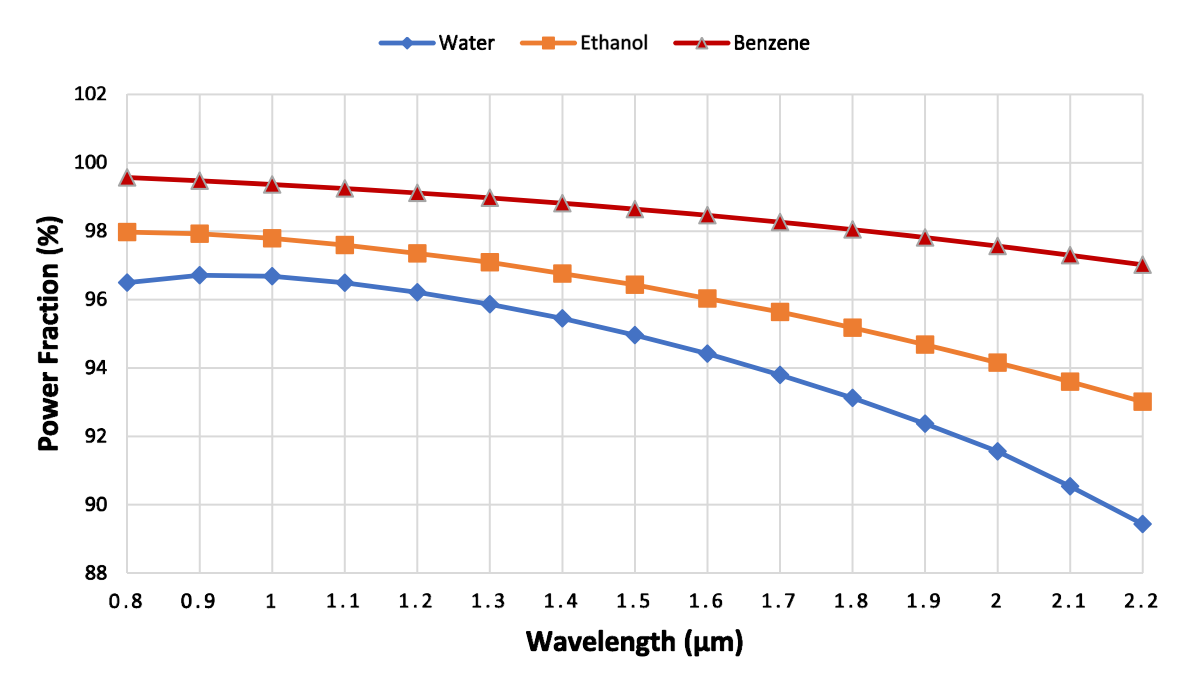


Figure 6: Changes in the power fraction of the fundamental x-polarized mode based on the wavelength for liquid analytes.

decreases with increasing wavelength, indicating less sensitivity to longer wavelengths. These findings can aid in designing and optimizing the PCF sensor for applications involving these liquids. At a wavelength of 1.3 μ m, the power fractions for water, ethanol, and benzene are 95.86, 97.10, and 98.98%, respectively, indicating that the sensor is susceptible to these substances. These findings are essential for various applications where detecting these substances is critical, such as environmental monitoring and medical diagnostics.

The power fraction trends show how sensitivity changes with wavelength and how to choose the best working point. Higher power fractions mean that more light is trapped in the core and reacting with the analytes that have been injected. This makes it easier to notice small changes in the liquids.

A graph in Figure 7 illustrates how the confinement loss of the suggested PCF varies with the wavelength for water, ethanol, and benzene. As the wavelength increases, the confinement loss for all three liquids increases, causing more light to pass through the cladding and leave the core. In comparison, benzene has a slightly lower confinement loss than ethanol and water.

At a working wavelength of 1.3 μ m, the confinement losses for water, ethanol, and benzene are measured to be 1.2×10^{-10} , 1.5×10^{-10} , and 1.0×10^{-10} dB/m, respectively. These values indicate the degree to which the PCF sensor

can prevent light from leaking out and provide confinement of the light within the core. Lower loss enables light to remain guided over longer distances with minimal leakage into the cladding. This allows more interactions with the infiltrated analytes, improving detection sensitivity. The results suggest that the proposed PCF sensor may be effective in detecting and analyzing the properties of water, ethanol, and benzene, and can potentially be useful in various sensing applications.

Figure 8 shows how the effective area of the proposed PCF changes regarding the wavelength. The effective area provides a numerical assessment of transverse electric fields that tend to increase as the operating wavelength increases. This is demonstrated by the moderate increase in effective area with increasing wavelength. In comparison to ethanol and water, benzene has the smallest effective area. At a wavelength of 1.3 µm, the practical areas for water, ethanol, and benzene are found to be 11.06, 11.11, and 10.42 µm², respectively. The effective area is crucial in determining the performance of the PCF, and a greater effective area usually results in a more sensitive sensor. A greater effective area facilitates enhanced interaction between the guided light and the surrounding medium or analyte under consideration. The heightened level of interaction leads to an improved sensitivity of the sensor, hence increasing its ability to promptly detect and respond to variations in the surrounding sensory environment.

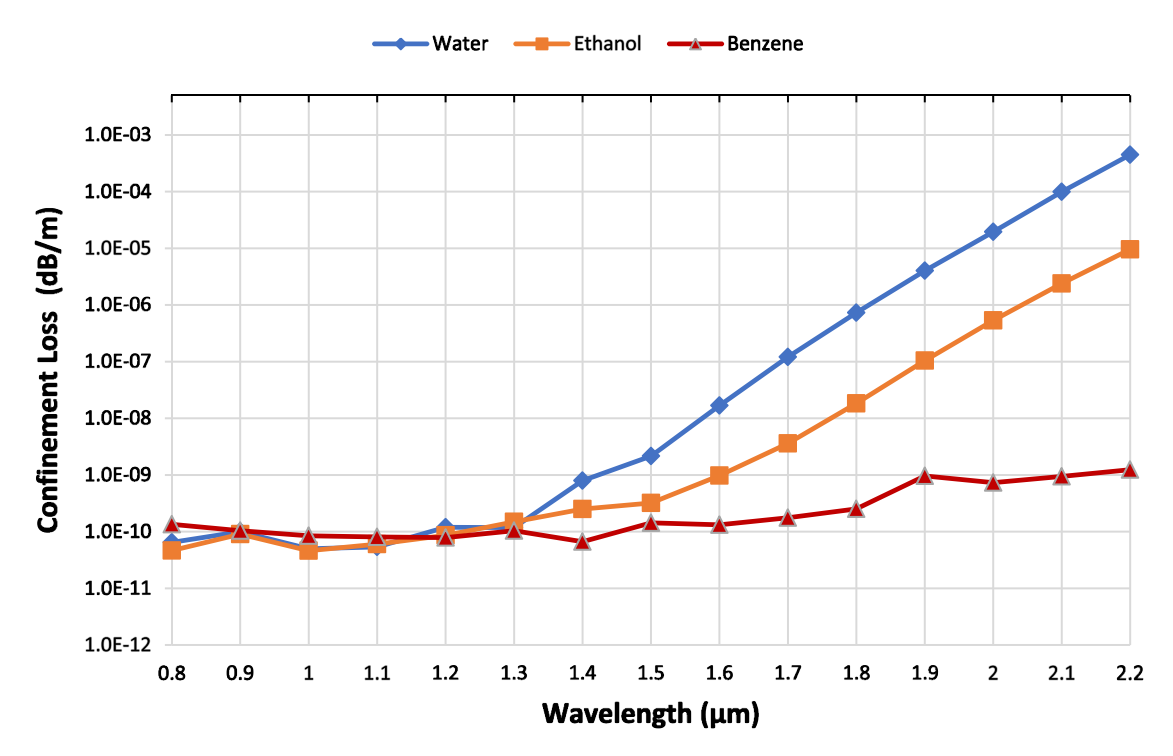


Figure 7: Changes in the confinement loss of the proposed sensor based on the wavelength for liquid analytes.

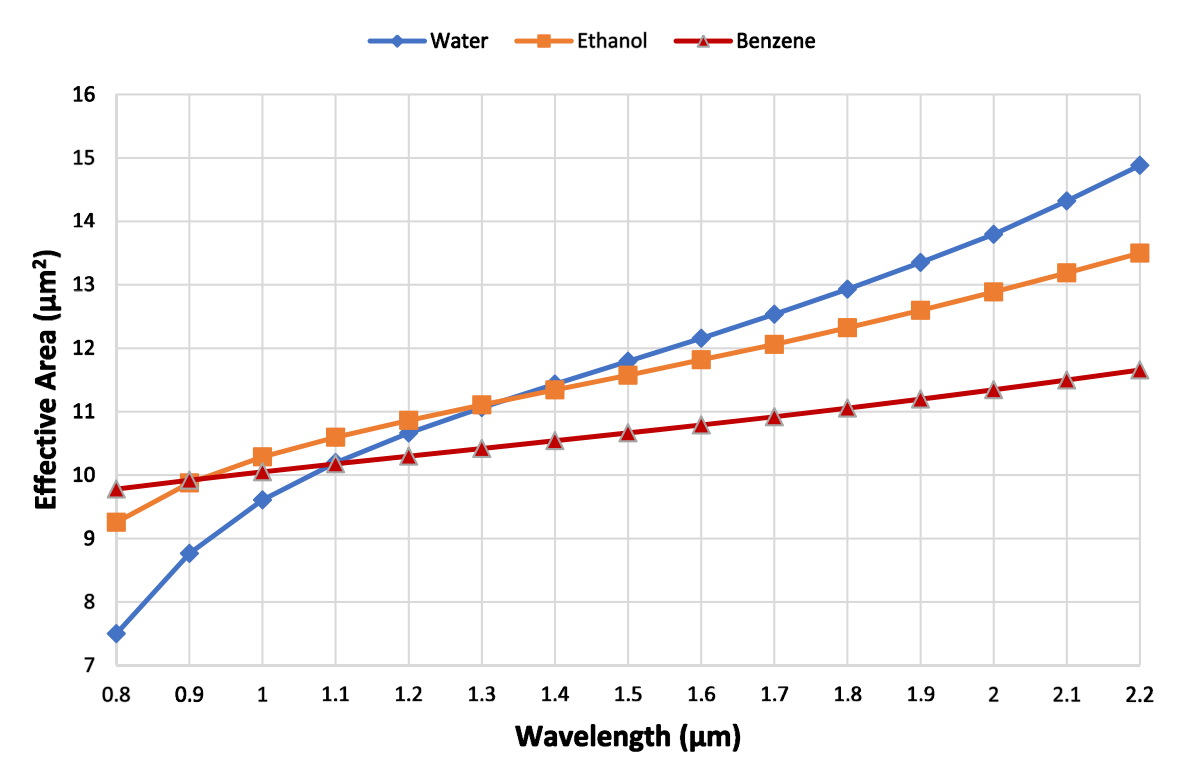


Figure 8: Changes in the effective area of the proposed sensor based on the wavelength for liquid analytes.

A graphical representation of the correlation between the nonlinear coefficient of the liquid analytes and the operating wavelength is presented in Figure 9. Water, ethanol, and benzene behave similarly, with the nonlinear coefficient decreasing as the operating wavelength increases. However,

there is a conflicting relationship between the nonlinear coefficient and the effective area, as illustrated in Figures 8 and 9. Despite this apparent conflict, the nonlinearity coefficients of water, ethanol, and benzene are almost identical at a wavelength of 1.3 μ m, with values of 13.98, 13.93, and 14.85

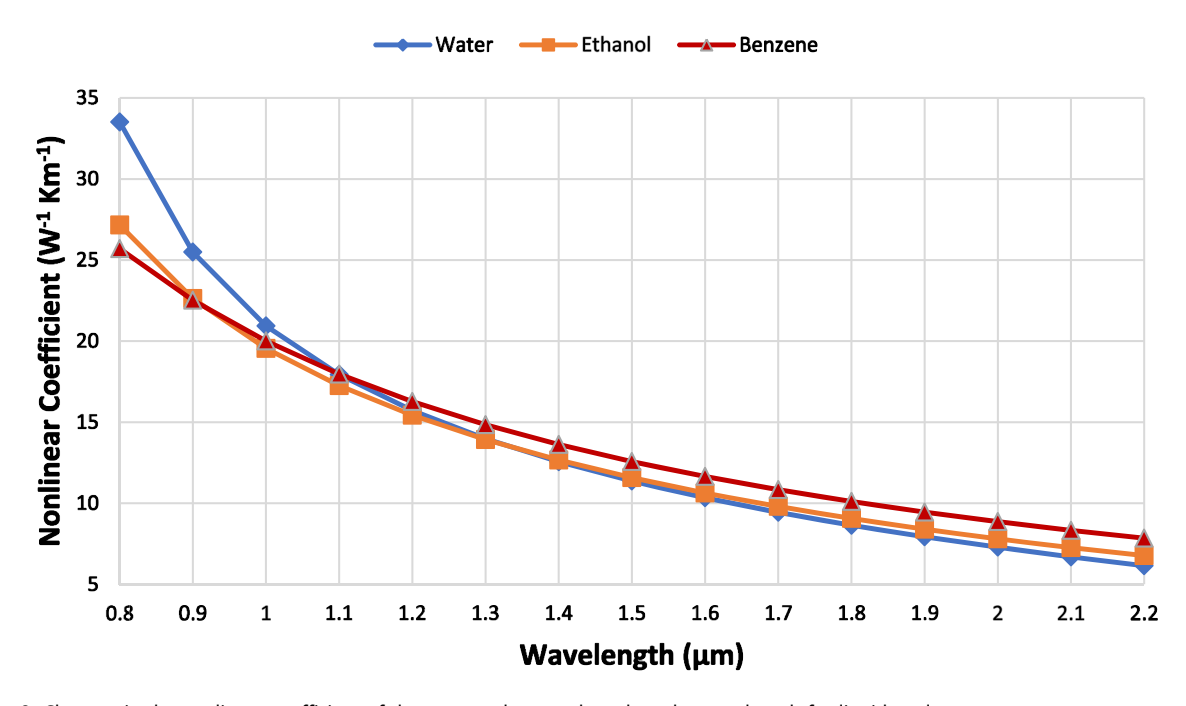


Figure 9: Changes in the nonlinear coefficient of the proposed sensor based on the wavelength for liquid analytes.

W⁻¹ km⁻¹, respectively. The presence of nonlinear effects may lead to the distortion of the transmitted light, potentially resulting in undesirable noise or measurement errors. Through the mitigation of these effects, PCF sensors can offer measurements that are both more precise and dependable.

The suggested PCF consists of a single core hole and five cladding air hole rings, and it was created with a reasonably basic design for use in liquid sensing applications. Using the current improvement in fabrication technology, creating with such a simple design is simple and inexpensive. Despite these benefits, it has been demonstrated that the suggested PCF's sensitivity is higher than that of many PCFs with more sophisticated designs, such as those provided in references [9,10,12–18]. It has lower confinement loss than most previous PCFs, making it suitable for liquid sensing. However, its confinement loss is slightly lower than reference [12] and comparable to those in references [9,10,13–18]. Despite these differences, the proposed PCF is still a good choice for the liquid sensing application.

Table 2 presents a comparison between the proposed PCF and previously investigated chemical PCF sensors. The results clearly indicate that the proposed PCF exhibits superior performance in terms of confinement loss and relative sensitivity. According to the data presented in the table, it can be observed that the suggested PCF sensor demonstrates the highest relative sensitivity when compared to other sensors. Additionally, it exhibits a low level of confinement loss.

Making complicated and simple PCF designs is now achievable because of technological advancements in manufacturing processes. The utilization of advanced manufacturing techniques such as stack and draw, drilling, sol–gel casting, and the extrusion method have been considered in the literature [32–35]. Design feasibility is an essential requirement for manufacturing the suggested PCF.

Furthermore, in relation to the construction of the suggested PCF sensor, a study was conducted to analyze the impact of deviations from the ideal specifications by varying the diameter of the cladding and core holes and the pitch size of the holes in the PCF design. This study is known as a tolerance study. In Table 3, with a wavelength of $\lambda = 1.3~\mu m$, an analysis of the proposed PCF caused by generic parameter changes in the order of ± 1 , ± 2 , and $\pm 3\%$ from the optimal values is shown. For deviations of up to $\pm 3\%$ from the ideal values, the changes in relative sensitivities are less than ± 1.3 , ± 1.2 , and $\pm 0.01\%$ for water, ethanol, and benzene, respectively, as shown in the data.

Similarly, confinement loss experiences minor changes of less than $\pm 5.5 \times 10^{-11}$, $\pm 1.1 \times 10^{-10}$, and $\pm 4.5 \times 10^{-12}\%$ for water, ethanol, and benzene, respectively. The nonlinear coefficient changes through less than ± 4.1 , ± 5.0 , and $\pm 5.4\%$ for water, ethanol, and benzene, respectively. Despite these discrepancies, it should be noted that the resulting confinement loss, nonlinear coefficient and relative sensitivity are still superior to those shown in Table 3.

Real-life operating conditions must be considered when moving PCF chemical sensors from computer simulations to real-world tests. These conditions can have a significant effect on the optical properties of the analyte and the measured sensor reaction. In particular, changing the temperature and pressure transforms the refractive index of specific analytes like benzene, water, and ethanol. To set a standard for this work, operation at room temperature (293.15 K) and atmospheric pressure (1 atm) are used for characterization and optimization. But to make the sensor technology work on a larger scale, it needs to be designed to resist environmental changes, or the system needs to be actively stabilized and calibrated. It is possible to lessen the effects of temperature and pressure-related changes in the refractive index by modeling the PCF sensor response across the expected

Table 2: The contrast between the suggested PCF and previously studied PCF sensors

PCF	Sensitivity (%)			Confinement loss (dB/m)			
	Water	Ethanol	Benzene	Water	Ethanol	Benzene	
Reference [12]	23.3	24.2	24.9	10 ⁻²	10 ⁻³	10 ⁻³	
Reference [10]	_	29	_	_	10 ⁻⁷	_	
Reference [9]	41.37	_	_	10 ⁻¹⁰	_	_	
Reference [13]	45.1	46.9	47.4	10 ⁻¹⁵	10 ⁻¹⁴	10 ⁻¹⁴	
Reference [14]	48.2	53.2	55.6	_	_	_	
Reference [15]	52.1	56.8	58.9	10 ⁻¹³	10 ⁻¹³	10 ⁻¹³	
Reference [16]	62.6	65.3	74.5	10 ⁻⁷	10 ⁻⁸	10 ⁻¹¹	
Reference [17]	88.9	91.9	97.9	10 ⁻¹⁰	10 ⁻¹⁰	10 ⁻¹⁰	
Reference [18]	94.5	96.3	99.6	10 ⁻⁹	10 ⁻¹⁰	10 ⁻¹³	
Proposed	96.84	98.12	100.00	10 ⁻¹⁰	10 ⁻¹⁰	10 ⁻¹⁰	

Table 3: Comparing how the global parameters change at the optimal parameters at $\lambda = 1.3 \ \mu m$

Change in global Parameters (%)	Relative sensitivity (%)			Confinement loss (dB/m)		Nonlinear coefficient (W ⁻¹ km ⁻¹)			
	Water	Ethanol	Benzene	Water	Ethanol	Benzene	Water	Ethanol	Benzene
+3%	97.06	98.44	100.00	3.7 × 10 ⁻¹⁰	7.6 × 10 ⁻¹⁰	7.3 × 10 ⁻¹⁰	9.70	8.93	9.09
+2%	96.98	98.32	100.00	1.8×10^{-10}	4.3×10^{-10}	5.5×10^{-10}	12.11	10.19	10.57
+1%	96.91	98.25	100.00	1.1×10^{-10}	2.4×10^{-10}	2.7×10^{-10}	10.72	11.82	12.44
Optimum	96.84	98.12	100.00	1.2×10^{-10}	1.5×10^{-10}	1.0×10^{-10}	13.98	13.93	14.85
-1%	96.76	97.90	100.00	9.9×10^{-11}	9.2×10^{-11}	8.5×10^{-11}	16.49	16.70	18.03
-2%	96.54	97.56	99.99	8.7×10^{-11}	7.2×10^{-11}	6.8×10^{-11}	19.85	20.39	22.35
-3%	96.42	97.13	99.93	7.8×10^{-11}	5.2×10^{-11}	4.0×10^{-11}	24.42	25.42	28.37

working parameter space and then optimizing the photonic crystal structure to match. It is easier to understand and demonstrate PCF chemical sensors when they are used in a lab with stringent controls, which is what is expected here. However, putting this technology into practice requires designs that can handle changes in the real world. This can be done through multi-physics models and engineered materials not sensitive to temperature or pressure.

4 Conclusion

The PCF is a recently proposed type of optical fiber that shows promise for use in liquid sensing in the lower optical wavelength range. Accurate identification and quantification of liquid samples are of utmost importance in various fields, such as environmental monitoring, industrial processing, medical diagnostics, and laboratory research. The novel fiber is structured with a single circular core hole and air holes in the cladding, arranged in a hybrid layout spanning five layers. This unique design allows for the effective and efficient detection of different liquids. To determine the characteristics of this new fiber, numerical simulations were conducted using the full vector FEM method. This technique is effective in studying the attributes of optical fibers, and it was employed to assess PCF's functionality regarding sensitivity, nonlinear coefficient, confinement loss, power fraction, and effective area. The fiber was tested with three different liquids: water, ethanol, and benzene. The results showed that the proposed PCF has high sensitivity and can detect water, ethanol, and benzene, with a sensitivity of 96.84, 98.12, and 100%, respectively, at an optimal wavelength of 1.3 µm. Furthermore, the nonlinear coefficient of PCF was observed to be 13.98, 13.93, and $14.85~\text{W}^{-1}~\text{km}^{-1}$ for water, ethanol, and benzene, respectively. The PCF showed good performance results in various characteristics, such as confinement loss, power fraction, and effective area. This means that the proposed fiber has the potential for various applications, including optical communication, chemical detection, and biosensing. Overall, the PCF is a promising innovation that can help advance the field of liquid sensing and pave the way for new technological applications.

Acknowledgements: The author would like to thanks Mustansiriyah University (www.uomustansiriyha.edu.iq) Baghdad, Iraq for its support in the present work.

Funding information: Authors declare that the manuscript was done depending on the personal effort of the author, and there is no funding effort from any side or organization.

Conflict of interest: The authors state no conflict of interest.

Data availability statement: Most data sets generated and analyzed in this study are comprised in this submitted manuscript. The other data sets are available on reasonable request from the corresponding author with the attached information.

References

- Reeves WH, Skryabin DV, Biancalana F, Knight JC, Russell PSJ, Omenetto FG, et al. Transformation and control of ultra-short pulses in dispersion-engineered photonic crystal fibres. Nature. 2003:424(6948):511-5.
- Bjarklev A, Broeng J, Bjarklev AS. Photonic crystal fibres. Berlin: [2] Springer Science & Business Media; 2003.
- Xu Z, Duan K, Liu Z, Wang Y, Zhao W. Numerical analyses of splice losses of photonic crystal fibers. Opt Commun. 2009;282(23):4527-31.
- Habib MA, Reza MS, Abdulrazak LF, Anower MS. Extremely high birefringent and low loss microstructure optical waveguide: Design and analysis. Opt Commun. 2019;446:93-9.

- [5] Abbott D, Zhang XC. Special issue on T-ray imaging, sensing, and retection. Proc IEEE. 2007;95(8):1509–13.
- [6] Morshed M, Hassan MI, Roy TK, Uddin MS, Razzak SMA. Microstructure core photonic crystal fiber for gas sensing applications. Appl Opt. 2015;54(29):8637–43.
- [7] Chang YH, Jhu YY, Wu CJ. Temperature dependence of defect mode in a defective photonic crystal. Opt Commun. 2012;285(6):1501–4.
- [8] Bock WJ, Chen J, Eftimov TW. A photonic crystal fiber sensor for pressure measurements. In: IEEE Instrumentation and Measurement Technology Conference Proceedings. IEEE; 1999; 2005. p. 1177.
- [9] Arif MFH, Hossain MM, Islam N, Khaled SM. A nonlinear photonic crystal fiber for liquid sensing application with high birefringence and low confinement loss. Sens Biosensing Res. 2019;22:100252.
- [10] Asaduzzaman S, Ahmed K. Microarray-core based circular photonic crystal fiber for high chemical sensing capacity with low confinement loss. Optica Applicata. 2017;47(1):41–9.
- [11] Miluski P, Kochanowicz M, Zmojda J, Silva AP, Reis PNB, Dorosz D. Carbon laminates with RE doped optical fibre sensors. Open Eng. 2016;6(1):385–8.
- [12] Ademgil H, Haxha S. PCF based sensor with high sensitivity, high birefringence and low confinement losses for liquid analyte sensing applications. Sensors. 2015;15(12):31833–42.
- [13] Ahmed K, Morshed M. Design and numerical analysis of microstructured-core octagonal photonic crystal fiber for sensing applications. Sens Biosensing Res. 2016;7:1–6.
- [14] Islam MS, Paul BK, Ahmed K, Asaduzzaman S, Islam MI, Chowdhury S, et al. Liquid-infiltrated photonic crystal fiber for sensing purpose: design and analysis. Alex Eng J. 2018;57(3):1459–66.
- [15] Ahmed K, Morshed M, Asaduzzaman S, Arif MFH. Optimization and enhancement of liquid analyte sensing performance based on square-cored octagonal photonic crystal fiber. Opt (Stuttg). 2017;131:687–96.
- [16] Maidi AM, Yakasai I, Abas PE, Nauman MM, Apong RA, Kaijage S, et al. Design and simulation of photonic crystal fiber for liquid sensing. Photonics. 2021 Jan;8(1):1–14.
- [17] Eid MMA, Habib MA, Anower MS, Rashed ANZ. Highly sensitive nonlinear photonic crystal fiber based sensor for chemical sensing applications. Microsyst Technol. 2021;27:1007–14.
- [18] Maidi AM, Shamsuddin N, Wong WR, Kaijage S, Begum F. Characteristics of ultrasensitive hexagonal-cored photonic crystal fiber for hazardous chemical sensing. In: Photonics. MDPI; 2022. p. 38.
- [19] Buczynski R. Photonic crystal fibers. Acta Phys Pol A. 2004;106(2):141–67.
- [20] Wang P, Farrell G, Semenova Y, Rajan G. Influence of fiber manufacturing tolerances on the spectral response of a bend loss based all-fiber edge filter. Appl Opt. 2008;47(16):2921–5.
- [21] Amouzad Mahdiraji G, Chow DM, Sandoghchi SR, Amirkhan F, Dermosesian E, Yeo KS, et al. Challenges and solutions in fabrica-

- tion of silica-based photonic crystal fibers: an experimental study. Fiber Integr Opt. 2014;33(1–2):85–104.
- [22] Lopato P, Herbko M, Mescheder U, Kovacs A. Influence of a thin dielectric layer on resonance frequencies of square SRR metasurface operating in THz band. Open Eng. 2023 Jan;13(1):1.
- [23] Lee HW, Schmidt MA, Uebel P, Tyagi H, Joly NY, Scharrer M, et al. Optofluidic refractive-index sensor in step-index fiber with parallel hollow micro-channel. Opt Express. 2011;19(9):8200–7.
- [24] Akowuah EK, Gorman T, Ademgil H, Haxha S, Robinson GK, Oliver JV. Numerical analysis of a photonic crystal fiber for biosensing applications. IEEE J Quantum Electron. 2012;48(11):1403–10.
- [25] Hossain M, Podder E, Adhikary A, Al-Mamun A. Optimized hexagonal photonic crystal fibre sensor for glucose sensing. Adv Res. 2018:13(3):1–7.
- [26] Yakasai IK, Abas PE, Ali S, Begum F. Modelling and simulation of a porous core photonic crystal fibre for terahertz wave propagation. Opt Quantum Electron. 2019;51:1–16.
- [27] Yakasai I, Abas PE, Kaijage SF, Caesarendra W, Begum F. Proposal for a quad-elliptical photonic crystal fiber for terahertz wave guidance and sensing chemical warfare liquids. In: Photonics. MDPI; 2019. p. 78.
- [28] Begum F, Abas PE. Near infrared supercontinuum generation in silica based photonic crystal fiber. Prog Electromagn Res C. 2019;89:149–59.
- [29] Begum F, Namihira Y, Kinjo T, Kaijage S. Supercontinuum generation in photonic crystal fibres at 1.06, 1.31, and 1.55 mm wavelengths. Electron Lett. 2010;46(22):1.
- [30] Kaijage SF, Ouyang Z, Jin X. Porous-core photonic crystal fiber for low loss terahertz wave guiding. IEEE Photonics Technol Lett. 2013;25(15):1454–7.
- [31] Benhaddad M, Kerrour F, Benabbes O. Design and analysis of nonlinear properties of photonic crystal fiber with Various Doping Concentration. In: Journal of Physics: Conference Series. IOP Publishing; 2018. p. 012010.
- [32] Kikuchi K, Taira K, Sugimoto N. Highly-nonlinear bismuth oxide-based glass fibers for all-optical signal processing. In: Optical Fiber Communication Conference. Optica Publishing Group; 2002. p. ThY6.
- [33] Broeng J, Mogilevstev D, Barkou SE, Bjarklev A. Photonic crystal fibers: A new class of optical waveguides. Opt Fiber Technol. 1999;5(3):305.
- [34] Petrovich MN, Van Brakel A, Poletti F, Mukasa K, Austin E, Finazzi V, et al. Microstructured fibres for sensing applications. In: Photonic crystals and photonic crystal fibers for sensing applications. SPIE; 2005. p. 78–92.
- [35] El Hamzaoui H, Ouerdane Y, Bigot L, Bouwmans G, Capoen B, Boukenter A, et al. Sol-gel derived ionic copper-doped microstructured optical fiber: a potential selective ultraviolet radiation dosimeter. Opt Express. 2012;20(28):29751–60.